Chapter 6

SYNAPTIC TRANSMISSION I

INTRODUCTION

The past several chapters have been concerned with the flow of current in neurons without considering in much detail how such currents are generated under physiological circumstances. This and the next two chapters will consider synapses, which are one of two biological sources of currents in neurons. Synapses are points of functional contact between two neurons or between a neuron and a different type of cell, such as a muscle or gland cell. Synapses, thus, are always formed by two elements, a presynaptic element and a postsynaptic element. Information usually – but not always – flow unidirectionally from the presynaptic element to the postsynaptic element.

The nature of synapses was a point of contention between Cajal and the reticularists. The reticularists believed that the nervous system was a reticulum of interconnected elements. It would, then, be possible for electrical currents to flow from one element to the other. Cajal, on the other hand, argued that nerve cells are isolated units. This requires some mechanism by which information can proceed from one neuron to the other. How this could happen was initially not obvious. However, J. Newport Langley showed that a plant substance similar to nicotine could ganglion could affect the activity of cells in the autonomic nervous system and subsequently suggested (Langley, 1906) that synaptic transmission involves a chemical step. Otto Loewi showed a little later that electrical stimulation of the vagus

nerve in frogs produced a chemical substance that modulated the rate at which the heart was beating. This substance turned out to be the small molecule, acetylcholine, leading to the hypothesis that synapses depend upon a form of chemical communication. Whether synaptic transmission is electrical or chemical in nature remained controversial until the 1950's when a combination of anatomical and physiological studies revealed that both forms of transmission occur. Cowan and Kandel (2001) have summarized the history of concepts of synaptic transmission.

ELECTRICAL SYNAPSES

Electrical synapses were first demonstrated in the crayfish nerve cord by Furshpan and Potter (1957). They were then described in the central nervous system of fishes by M. V. L. Bennett and his colleagues (Bennett, 1972). They used a combination of electrophysiology and electron microscopy to show that gap junctions are the anatomical substrate for electrical synapses. Electrical synapses are widespread in invertebrate nervous systems, but were for some time held to be rare in vertebrate nervous systems. However, it has become clear over the past several years that electrical synapses are also found throughout the brains of vertebrates (Connors and Long, 2004).

Gap junctions are membrane specializations that establish continuity between two cells (Fig. 6-1). They are formed by membrane structures called connexons. Connexons are inserted into the membranes of the two apposed cells so that a pore is formed through the membrane of each cell. lons in one cell can, thus, pass through the pore into the adjacent cell.

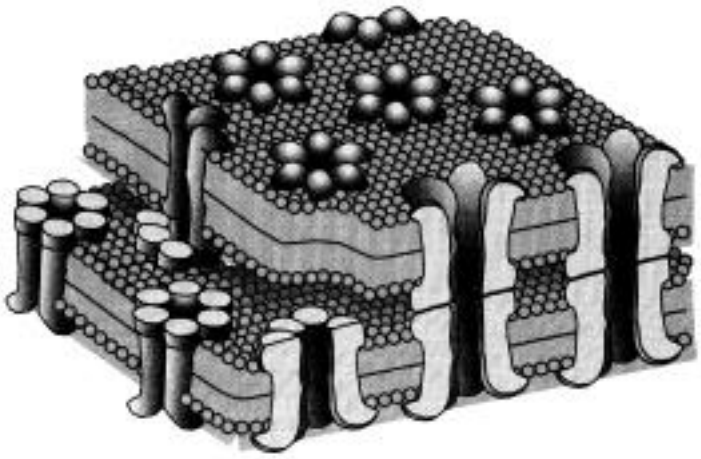

Figure 6-1. Gap junctions. Patches of the membranes of two cells conncected by gap junctions are shown. Connexxons form pores that connected the cytoplasms of the two cells. Each connexion is composed of twelve connexxins, six in the membrane of each cell.

Connexons are formed from proteins in a family called connexins. Each connexon is formed from six connexins. There are at least 40 varieties of connexins, which are named according to their molecular weights. Connexins with molecular weights of 36 kilodaltons, etc. Connexin Cx 36, Cx 45 and Cx 47 are particularly prevlent in the nervous systems of mammals.

The definitive physiological demonstration of electrical synapses requires recording simultaneously from the two connected cells. Passing a current into one cell, the presynaptic cell, produces a voltage transient or action potential in that cell and also produces a voltage transient in the presynaptic cell (Fig. 6-2). The latency between the voltage transient in the presynaptic cell and the transient in the postsynaptic cell has a latency of only tens or a hundred μs. Current can normally pass in both directions so that electrical synapses are said to be non-rectifying, in contrast to the properties of chemical synapses, which require that information flows from

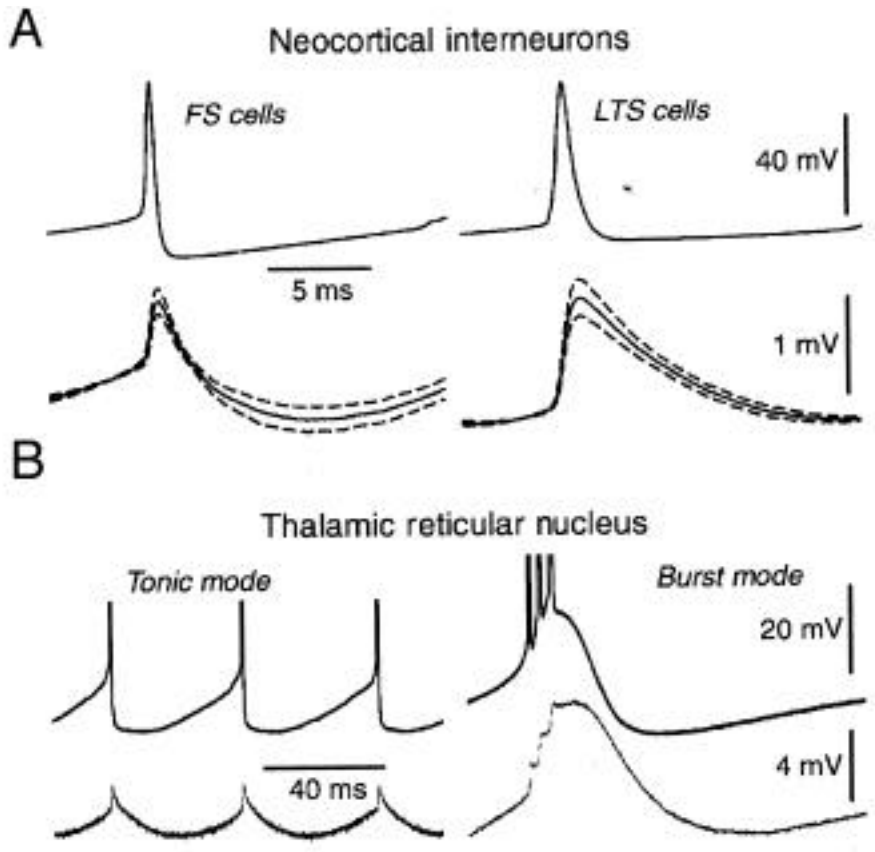

Figure 6-2. Elecrical synapses. This figure shows three examples of electrical synapses in mammalian brains. The top traces in each case show action potentials recorded in the presynaptic cell. The bottom traces shows electrical PSPs recorded in the postsynaptic cell. A. Two examples of electrical synapses in neocortical interneurons. B. Electrical synapses in cells in the thalamic reticular nucleus recorded when the presynaptic cell was in two different firing modes. From Connors and Long (2004).

the presynaptic to the postsynaptic element in the synapse. Electrical synapses are essentially resistors, so the current passing through the synapse can be represented, as a first approximation, by Ohm's law

(6-1) $$I_{syn} = g_{syn}[V_1 - V_2]$$

where I_{syn} is the current passing through the synapse, g_{syn} is the conductance of the synapse and $[V_1 - V_2]$ is the potential difference between

the two cells. Electrical synapses formed by Cx 36 have conductances of about 10 – 15 pS. Current flow between cells linked by electrical synapses can be more complicated, however, in that the conductance of the synapse can actually be a function of the voltage difference between the two cells. Two cells that are linked by a jap junction can be represented exactly as we represented two compartments in Chapter 3. If we represent the membrane potentials of cells 1 and 2 as the differences between their instantaneous membrane potentials and resting membrane potentials, then the membrane equation for cell 1 is

(6-2) $$-C_1 \frac{dV_1}{dt} = \frac{V_1}{R_1} + g_{syn}[V_1 - V_2]$$

where C_1 and R_1 are the capacitance and resistance of cell 1. The derivative vanishes at steady state, so if we substitute $R_{syn} = 1/g_{syn}$ and rearrange the equation we obtain an expression for the voltage of cell 1 as a function of cell 2:

(6-3) $$V_1 = \frac{R_1}{R_1 + R_{syn}} V_2 \quad .$$

Electrical synapses appear to have a considerable variety of functions. The first is that they are prevalent in situations in which synaptic transmission needs to be fast and reliable. We will se below that chemical synapses are complex entitites that transmit information relatively slowly and operate on a statistical basis. Thus, electrical synapses are commonly encountered in escape systems that allow an organism to rapidly evade a potential predator. They are also common in the auditory system and in

electrocommunication systems in which the transmission of information from one cell to the next must be very rapid in order to preserve the fidelity of the signal. It is becoming clear in recent years that electrical synapses are frequently involved in synchronizing the activity of networks of cells that oscillate at particular frequencies. There are also mixed synapses in which a given synaptic element forms both an electrical synapse and a chemical synapse. This provides for a rapid transmission of information between the two connected cells that is followed by a slower transmission.

The activity of electrical synapses can often be modulated by a variety of factors that include temperature, pH of the extracelluar space and the activity of other cells, such as dopaminergic cells in the retina.

CHEMICAL SYNAPSES

Our basic concepts of the function of chemical synapses comes from the work of Sir Bernard Katz, José DelCastillo and Ricardo Miledi, who used the synapses of spinal motor neurons onto frog leg muscles to develop a model of synaptic mechanisms (Katz, 1969). The contribution that Katz and his colleagues made to our understanding of synaptic function was to show how synaptic transmission is probabilistic, or stochastic, in nature. Their work was based on experiments carried out on the neuromuscular junctions of frogs. We will start our discussion of chemical synapses by considering the neuromuscular junction and Katz's work, and then seeing how this basic model of synaptic transmission can be extended to central synapses.

Anatomy of the neuromuscular junction

The neuromuscular junction is a large synapse effected by spinal motoneurons upon striated muscle fibers, such as the *sartorius muscle* of the leg. Because it is large, it is easy to work with and has been studied extensively with the electron microscope and tools from molecular biology. We now know a great deal about neuromuscular junctions (Fig. 6-3) in a range of animals (Hoyle, 1983). In vertebrates, neuromuscular junctions occur as small clusters of synaptic boutons on the ends of motoneuron axons or as large and elongate synaptic terminals. The first type of endings are called *en grappe* endings and the second are called *en plaque* endings. Both types use an excitatory neurotransmitter which is either acetylcholine or a closely related compound. The larger *en plaque* endings are the best studied (Fig. 6-4). They contain thousands of clear, round synaptic vesicles and a smaller number of larger vesicles with dense cores. The small vesicles contain acetylcholine and the large vesicles contain neuroactive peptides.

The synaptic terminal is the *presynaptic element* in the synapse in the sense that information is flowing from it to a muscle cell, which is the *postsynaptic element*. The plasma membrane of the terminal facing the synapse is called the *presynaptic membrane* (Fig. 6-5). It contains bar-shaped protein complexes arranged perpendicular to the long axis of the terminal. These are composed of a variety of proteins that help to control the release of synaptic vesicles and neurotransmitter by the terminal. The bars are *active zones*. As the terminal is activated by an action potential in the presynaptic axon, vesicles that have been guided to the active zones by the cytoskeleton of the terminal fuse with the presynaptic membrane and

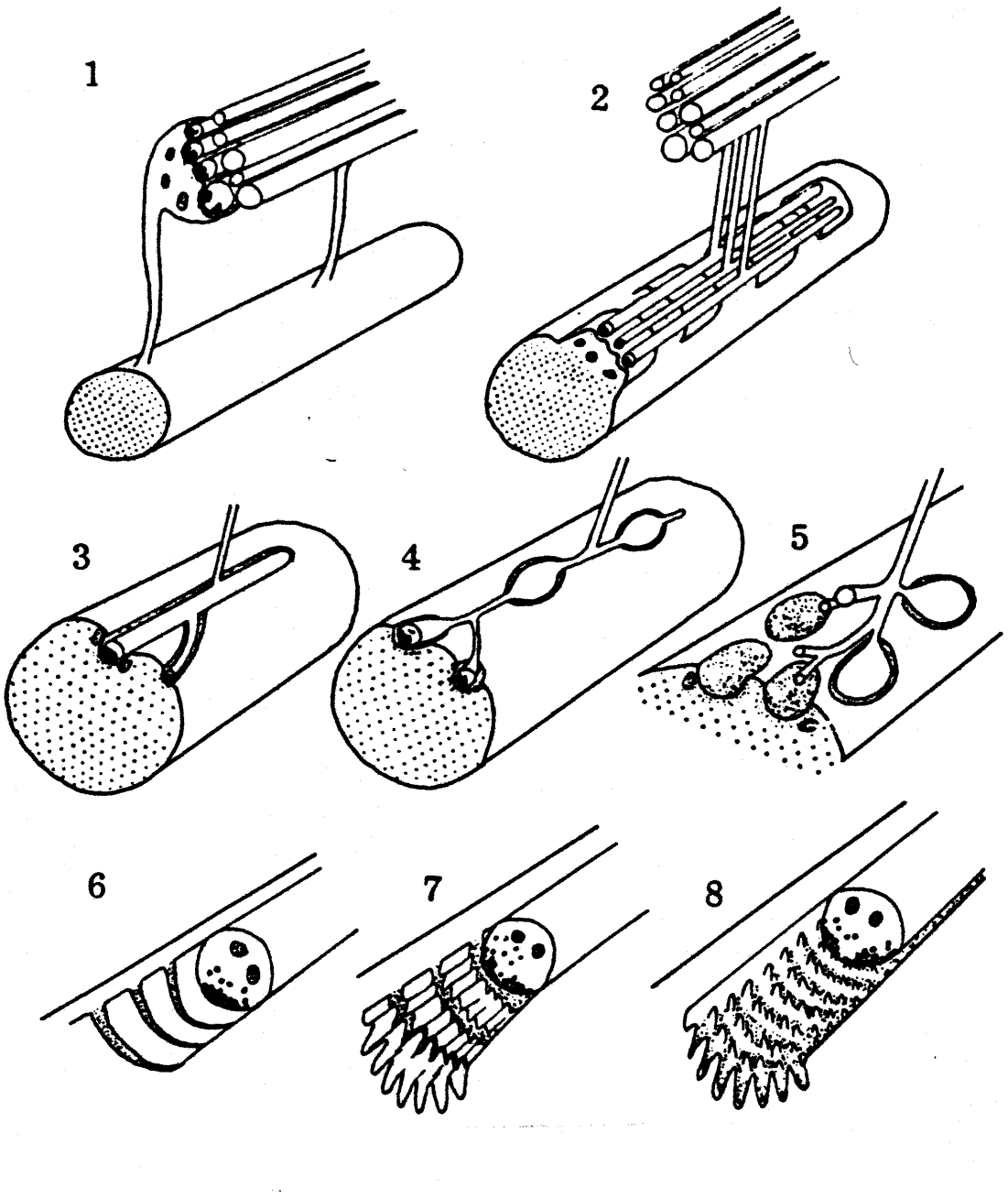

Figure 6-3. Neuromuscular junctions. Neuromuscular junctions from a variety of animals. 1. Muscle cell has a process that contacts nerve (many invertebrates). 2. Short pillar extends from muscle cell to contact nerves (annelids, molluscs, insects). 3. Nerve branches fit into muscle cell (arthropods, molluscs, annelids, fish). 4. Nerve has varicosities that fit into muscle (crustaceans, insects, molluscs, fish). 5. *En grappe* ending on vertebrate slow muscle. 6. Muscle cell has a groove with transverse infolding (amphibians). 7. Muscle cell has groove with both longitudinal and transverse foldings (reptiles). 8. Muscle cell has a highly folded groove (mammalian fast muscles). From Hoyle (1983).

release their contents into the *synaptic cleft* that separates the axon terminal from the postsynaptic membrane of the muscle cell. The synaptic cleft in neuromuscular junctions contains a feltwork of connective tissue molecules called the *basal lamina*. Acetylcholine released by the presynaptic terminal diffuses through the basal lamina and binds to *acetylcholine receptors*. Like most ligand-gated receptors, those that bind acetylcholine come in more than one variety. The receptors found in the neuromuscular junction interact with the compound nicotine and are called *nicotinic acetylcholine receptors*. They are large protein complexes that are inserted into the membrane of the muscle cell beneath the active zones of the presynaptic terminal. Each receptor is composed of five individual protein molecules, called *receptor subunits,* arranged around a central pore. The conformation of the subunits is normally such that the pore is occluded and ions cannot pass between the synaptic cleft and the interior of the muscle cell. However, the conformation quickly changes when the synapse is activated and ions can flow through the pore if two molecules of acetylcholine bind to two of the receptor subunits. This is a source of a PSC in the postsynaptic membrane.

In principle, the acetylcholine molecules could stay bound to the receptor subunits forever and current would continue to flow, forcing the muscle fibers into a state of perpetual contraction. However, several factors mitigate against this. The first is that the affinity of the receptor subunits to acetylcholine is low enough for there to be a significant probability that the two acetylcholine molecules will be released by the subunits. Second, the synaptic cleft is open to the extracellular space surrounding the terminal, so acetylcholine begins diffusing out of the

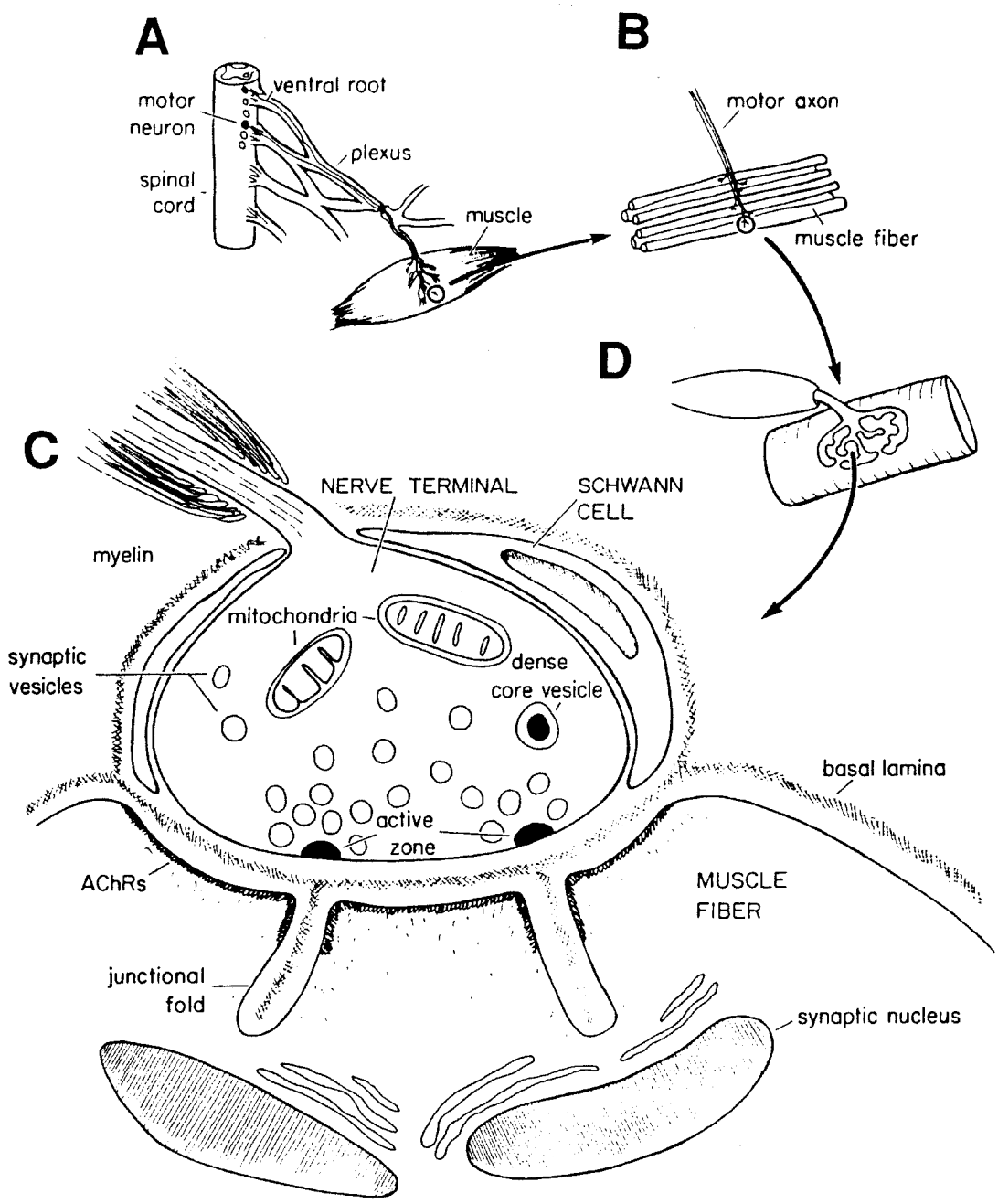

Figure 6-4. Vertebrate neuromuscular junction. A. spinal cord with a spinal nerve that innervates a striated muscle. B. Magnified view of the motor axons innervating muscle fibers. C. Magnified view of an individual neuromuscular junction contacting a single fiber. D. Ultrastructural view of an axon innervating a single muscle fiber. From Hall and Sanes (1993).

synaptic cleft as soon as it is released by a vesicle. Third, the basal lamina contains molecules of an enzyme, *acetylcholinesterase*, that degrades acetylcholine. Release of acetylcholine by one or more vesicles produces a short-lived pulse of transmitter in the synaptic cleft.

The process of vesicle release can be studied easily using the frog neuromuscular junction because a leg muscle with a piece of the nerve attached can be removed from the frog and maintained in a solution (Ringer's solution) with the appropriate mix of ions. The nerve can be electrically activated, causing action potentials to invade the presynaptic terminal and trigger the release of transmitter into the cleft. The outcome of the release is monitored by inserting a recording electrode near the terminal and recording the resulting EPSPs, which are called *excitatory junction potentials* (EJPs) or *end plate potentials* (EPPs) in this case (Fig. 6-6). Since the electrode is close to the source of the current, electrotonic filtering by the membrane of the muscle cell is minimal. Since the preparation is in Ringer's solution, the ionic composition of the bath can be altered. This is important because vesicle release depends upon the proper concentration of extracellular calcium and the rate of vesicle release can be modulated by altering the calcium concentration in the Ringer's solution. What Katz and his co-workers did was to stimulate the motoneuron axon and record the resulting trains of EPPs in the muscle cell. They found noticeable variations in the amplitudes of the EPPs. This led to a theoretical formulation of the mechanisms of vesicle release which can be called the *Katz theory* (Stevens, 1993).

Digression on probability and statistics

Before considering Katz's theory in detail, it will be helpful to first introduce some basic concepts from probability and statistics. The data sets we are dealing with consist of trains of EPPs that vary in amplitude. It is natural to quantify this variability by measuring the amplitudes and constructing a *histogram* or bar graph to display the results. If the EPPs varied in amplitude between 0.0 mV and 1.0. mV, they could be categorized into 0.1 mV bins and used to construct a histogram showing the number of EPPs with amplitudes that fall within each bin (Fig. 6-6B, C). The histogram can be characterized by two descriptive statistics, the *mean* and *standard deviation*. The mean is also called the the arithmetic average of the data and is obtained by multiplying the number of PSPs with a given amplitude by the amplitude, adding all of these values together and then

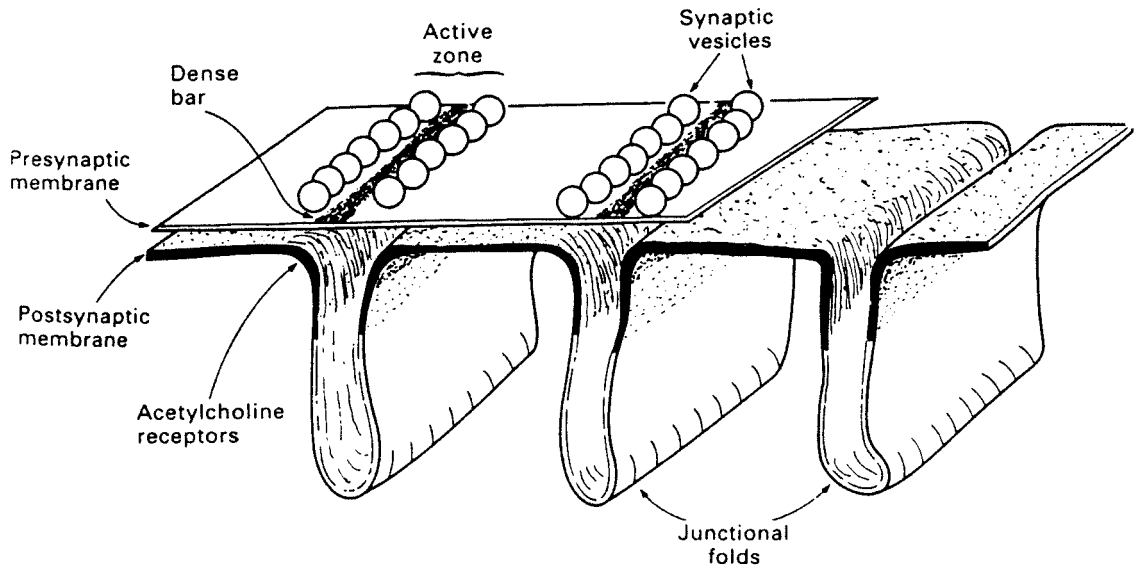

Figure 6-5. Synaptic membranes in a vertebrate neuromuscular junction. Highly magnified view of the presynaptic and postsynaptic membranes that form a neuromuscular junction. From Aidley (1989).

dividing them by the total number of PSPs in the sample. If the PSPs have amplitudes of x_1, x_2, ..., x_i, ... x_k and the number of PSPs with a given amplitude is n_1, n_2 , ..., n_i, ..., x_k, then the mean amplitude, $\bar{x}$, is given by

(6-4) $$\bar{x} = \frac{1}{N}\sum_{i=1}^{k} n_i x_i$$

where

(6-5) $$N = \sum_{i=1}^{k} n_i \quad .$$

The variance, $\mathrm{var}\{x\}$, is the average deviation from the mean. It is calculated by subtracting each amplitude from the mean value, squaring to get rid of minus signs and taking the sum

(6-6) $$\mathrm{var}\{x\} = \frac{1}{N}\sum_{i=1}^{k} (\bar{x} - x_i)^2 n_i \quad .$$

The standard deviation, σ, is the square root of the variance

(6-7) $$\sigma = \sqrt{\mathrm{var}\{x\}} \quad .$$

It is often convenient to construct a *frequency histogram*, which can be done by calculating the frequency or $f_i = n_i / N$ for each amplitude value and using frequencies, rather than numbers, to make the histogram. The formulae for the mean and variance of the data set are then

(6-8) $$\bar{x} = \sum_{i=1}^{k} f_i x_i$$

and

(6-9) $$\mathrm{var}\{x\} = \sum_{i=1}^{k} (\bar{x} - x_i)^2 f_i \quad .$$

The frequency histogram corresponds to the mathematical concept of a *probability density function,* $f(x)$*,* which gives the probability of finding a particular value, x_1, of the random variable, x, (Fig. 6-7 A). An important feature of such distributions is that the probability of x assuming values in the interval $x_1 \le x \le x_2$ is given by the area under the density function between x_1 and x_2, which is

(6-10) $$\mathrm{Prob}\{x_1 \le x \le x_2\} = \int_{x_1}^{x_2} f(x)dx \quad .$$

The area under the entire curve is always 1 because the probabilty of x falling between ±∞ is always 1. The probability density function is a function of a continuous variable in this case, but probability density functions can also be defined for variables that take on discrete values. The integrals are replaced by sums in that case. The mean and variance are given in terms of integrals

(6-11) $$\bar{x} = \int_{-\infty}^{+\infty} f(x)xdx$$

and

(6-12) $$\mathrm{var}\{x\} = \int_{-\infty}^{+\infty} f(x)(\bar{x} - x)^2 \, dx \quad .$$

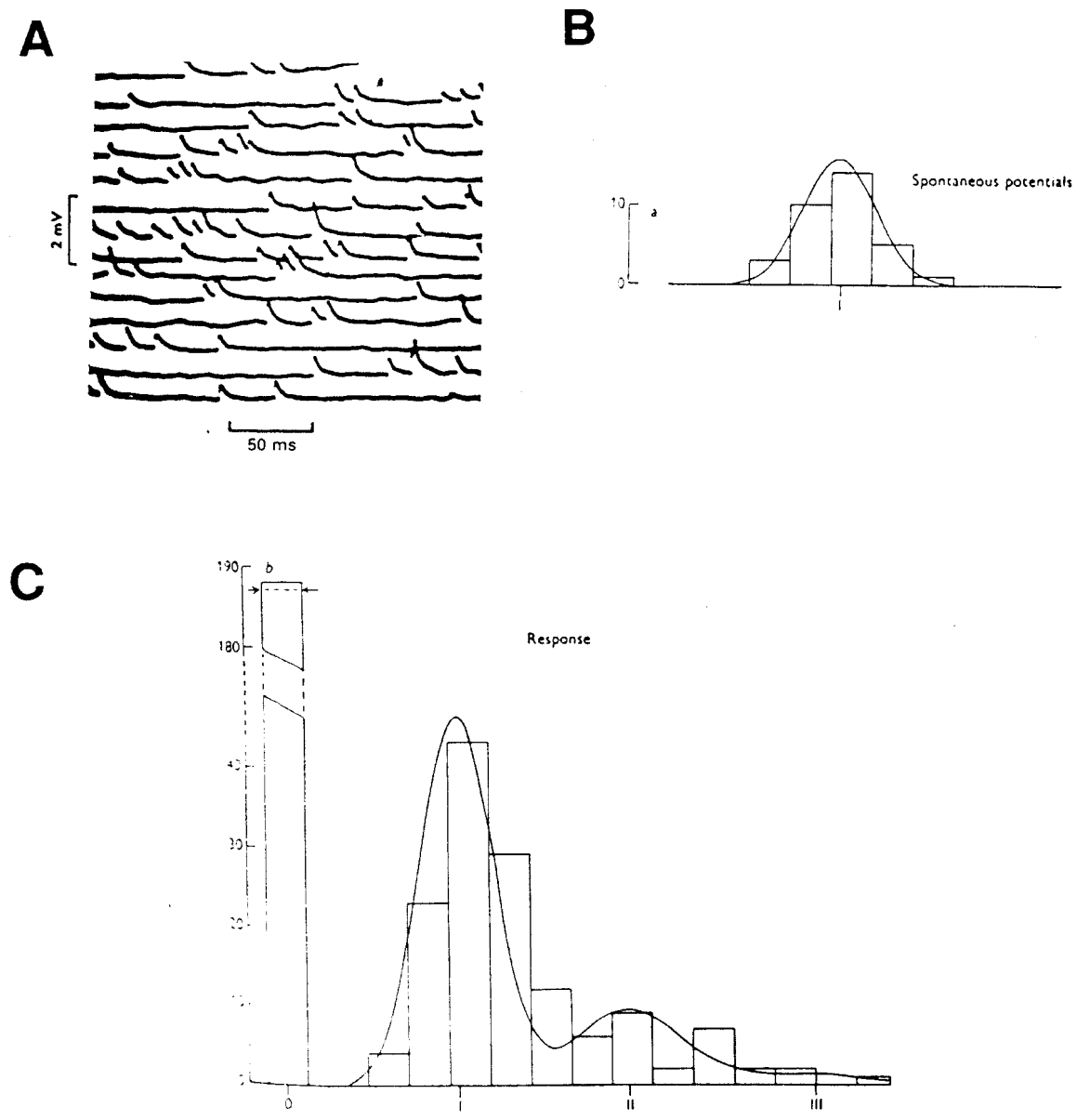

Figure 6-6. Endplate potentials. A. Samples of endplate potentials (EPPs) recorded from the sartorius muscle of a frog. From Fatt and Katz (1952). B. Amplitude histogram of spontaneous EPPs. The histogram is fit with a single Gaussian function. B. Amplitude histogram of evoked EPPs. Notice the large number of failures, represented by EPPs with 0 amplitude. The histogram is fit with a sum of two Gaussian functions. From del Castillo and Katz (1954).

The mean of a variable is often called the *expected value*, $E\{x\}$, of the variable, so $\bar{x} = E\{x\}$ and $\sigma^2 = E\{(x - \bar{x})^2\}$.

A concept related to the probability density function is the *cumulative distribution function* (Fig. 6-6B), which is the probability of x having a value less than or equal to some particular value. It is given by the integral

(6-13) $$F(x_1) = \int_{-\infty}^{x_1} f(x)dx = \Pr ob\{x \leq x_1\}$$

Plots of cumulative distribution functions always begin at 0 and increase monotonically to 1. The probability density function for a distribution is the derivative of the cumulative distribution function.

Several probability density functions occur commonly and deserve to be commited to memory (Fig. 6-8). A simple probability density function is the *exponential distribution*

(6-14) $$f(x) = \lambda e^{-\lambda x}$$

where the parameter λ is a constant and the function is defined over the interval $x \geq 0$. To find the expected value of the distribution, we evaluate the integral

(6-15) $$E\{x\} = \int_0^{+\infty} xf(x)dx = \int_0^{+\infty} x\lambda e^{-\lambda x} dx \quad .$$

Integrate by parts and find that

(6-16) $$E\{x\} = x(-e^{-\lambda x})\Big|_0^{\infty} - \int_0^{\infty}(1)(-e^{-\lambda x})dx = \frac{1}{\lambda}$$

To find the variance, evalute the integral

(6-17) $$Var\{x\} = \int_0^{+\infty}(\bar{x} - x)^2 f(x)dx = \int_0^{+\infty}(\bar{x} - x)^2 \lambda e^{-\lambda x}dx \quad .$$

This is a bit more work, but it can be shown that

(6-18) $$Var\{x\} = \frac{1}{\lambda^2} \quad .$$

Perhaps the best known probability density function is the *bell-shaped curve* which is called a *normal* or *Gaussian distribution* after the German mathematician Karl Friedrich Gauss. It is given by the equation

(6-19) $$f(x) = \frac{1}{\sigma\sqrt{2\pi}}\,Exp\left[\frac{-(\bar{x} - \mu)^2}{2\sigma^2}\right] \quad .$$

The parameter μ specifies the midpoint of the distribution and corresponds to its mean. This can be shown by evaluating the integral

(6-20) $$\int_{-\infty}^{\infty}\frac{x}{\sigma\sqrt{2\pi}}\,Exp\left[\frac{-(\bar{x} - \mu)^2}{2\sigma^2}\right]dx = \mu \quad .$$

The parameter σ is the standard deviation and is a measure of the width of the distribution. This can be shown by evaluating the integral

(6-21) $$\int_{-\infty}^{\infty} \frac{(\bar{x}-\mu)^2}{\sigma\sqrt{2\pi}} Exp\left[\frac{-(x-\mu)^2}{2\sigma^2}\right] dx = \sigma^2 \quad .$$

The cumulative distribution function for the Gaussian distribution is called the *error function* and is given by the integral

(6-22) $$erf(x) = \int_{-\infty}^{x} \frac{1}{\sigma\sqrt{2\pi}} Exp\left[\frac{-(x-\mu)^2}{2\sigma^2}\right] dx \quad .$$

Values for the error function are given in standard mathematical tables and are presented as a subroutine in software packages. You can do calculations in terms of error functions without actually having to enter the functions into your work yourself; the software package does it for you.

Two discrete distributions are important for understanding synaptic transmission. One is the *Poisson distribution*, named after the French mathematician. Distributions for discrete random variables are given by *probability mass distribution functions*. The probability mass function for the Poisson distribution is given by

(6-23) $$f(x) = \frac{k^x}{x!} e^{-k}$$

where $x! = x(x-1)(x-2)...1$ and 0! = 1. This distribution is characterized by the parameter, k, which is both the mean and variance. The second discrete distribution is the *binomial distribution.* It describes the probabilities involved in flipping coins, which can have values of either heads or tails. If there are

n coins, the probability of flipping all of the coins and finding x heads and $n-x$ tails is

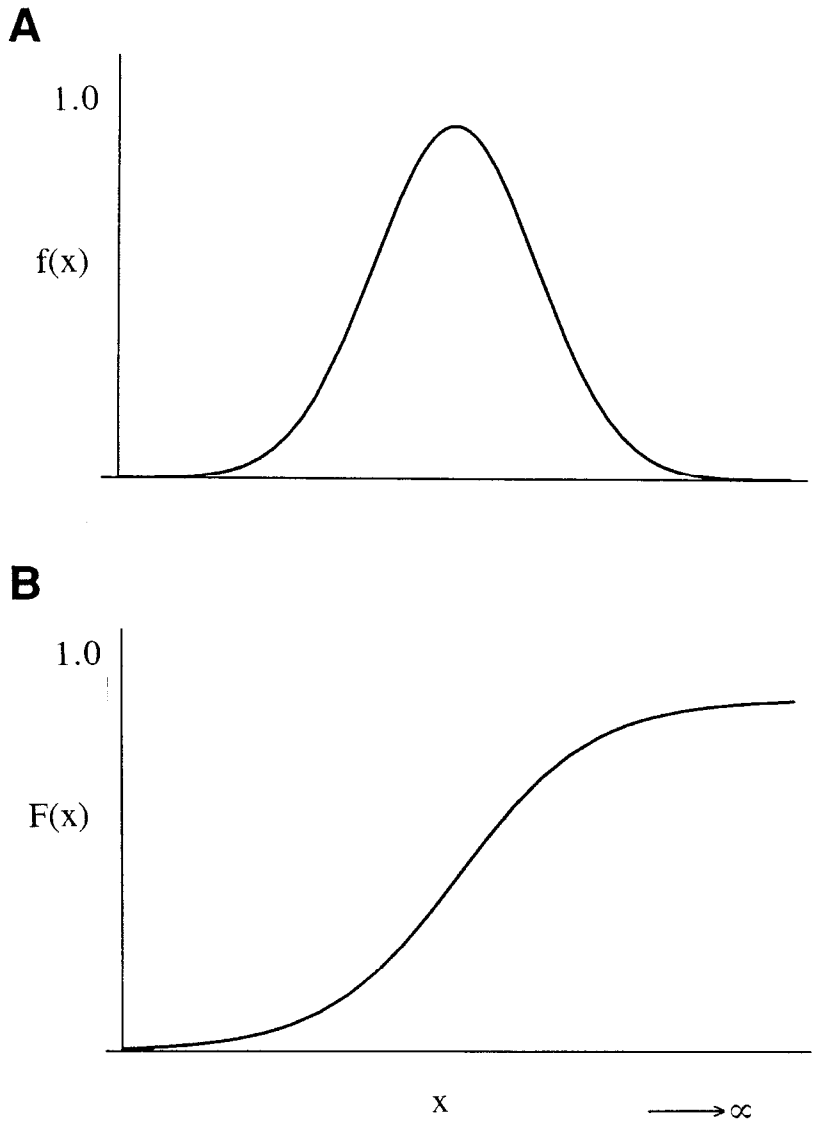

Figure 6-7. Probability density and cumulative distribution functions.
A. Probability density function, f(x), of the random variable, x. B. Cumulative distribution function, F(x), of the random variable, x.

(6-24) $$p(x) = \frac{n!}{(n-x)!\,x!}\,p^{x}(1-p)^{n-x}$$

where p is the probability of flipping the coin and getting a head.

The Katz theory

This digression on probability distributions allows us to follow the analysis of variations in EPP amplitude data carried out by Katz and co-workers (Fig. 6-6). One important result was obtained by removing calcium from the Ringer's solution. Calcium is required in the presynaptic terminal for action potentials to trigger vesicle release. Removing extracellular calcium blocks the release of vesicles evoked by electrical stimulation of the presynaptic axon and one might expect to see a complete absence of EPPs. Removing extracellular calcium greatly reduces, but does not completely eliminate EPPs. The amplitudes of such *spontaneous EPPs* were noticeably smaller than of *evoked EPPs* and they were consequently called *miniature EPPs*, "minis" or mEPPs. mEPPs did not all have exactly the same amplitude. Rather, mEPP amplitudes had a Gaussian distribution. A second important finding was obtained with low concentrations of calcium in the bath solution. This allows action potentials to evoke vesicle release, but reduces the number of vesicles released. Histograms of the amplitudes of evoked EPPs show several distinct peaks which can be fit by a sum of several Gaussian distributions (Fig. 6-6C). The mean of each distribution corresponds to one of the peaks. A striking finding was that the peaks occur at integer multiples of the amplitudes of the mEPPs. If the mean mEPP amplitude is 0.2 mV, then the other peaks occur at 0.4 mV, 0.6 mV, etc. The

frequencies of successive peak values show a distinct pattern in that they follow a Poisson distribution. The interpretation Katz and colleagues placed on this experiment was that transmitter is released in *quanta* corresponding to individual synaptic vesicles. mEPPs recorded in zero calcium result from spontaneous events in which a single vesicle fuses with the presynaptic membrane and releases its transmitter. There is some variance in mEPP amplitudes due to variations in the amount of transmitter packaged in different vesicles, size of vesicles, etc. Electrical activation in low calcium solution elicits the release of a vesicle with probability, p. Since p is relatively small in low calcium, release follows a Poisson distribution with the probability of x vesicles being released given by

(6-25) $$p(x) = \frac{m^x e^{-m}}{x!}$$

where m is the parameter that specifies the shape of the distribution. The expected value or mean of the distribution is $E\{x\} = m$. A presynaptic terminal that has n vesicles available for release with probability, p, will release, on average, $m = np$ vesicles. This is called the *mean quantal conten*t. Notice that there is some probability that the synapse will "fail" and no vesicles will be released. This occurs when $x = 0$, so $p(0) = m^0 e^{-m}/1 = e^{-m}$ and $m = -\ln p(0)$. Consequently, the mean quantal content can be conveniently estimated by counting the number of failures, an approach that is called the *method of failures*.

This formulation assumes that some number of vesicles is released simultaneously when the axon terminal is activated by invasion of an action potential. However, it is certainly the case that vesicle release occurs over

some small, but finite time window, under physiological conditions. This window is probably on the order of several hundred microseconds. The original Katz theory has been extended to take into account continuous release of vesicles using the concept of a *Poisson process* (Katz and Miledi, 1966; Barrett and Stevens, 1972,a,b). The probability of an event, such as release of a vesicle, is assummed to be proportional to the duration of the time window. The probability that an event occurs between time t and $t + dt$ is wdt, where w is the *Poisson rate*. This rate varies during the time over which the presynaptic terminal is releasing vesicles from a very low level prior to activation to a higher level as calcium enters the terminal.

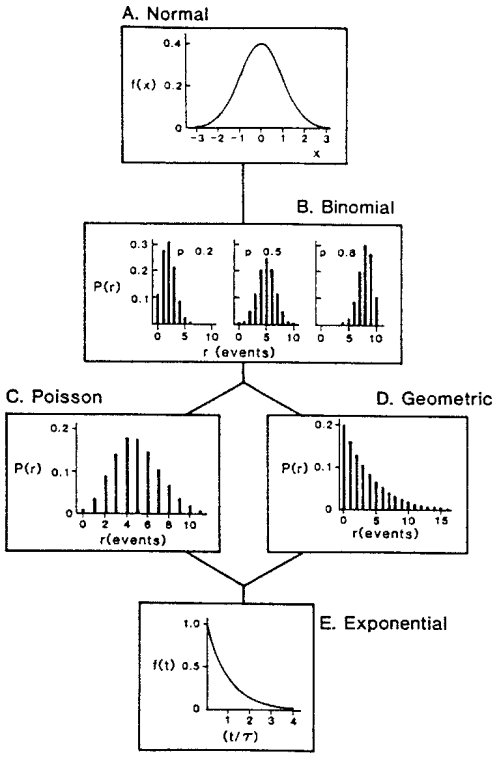

Figure 6-8. Commonly encountered probability density functions. Five commonly encountered probability density functions are shown. The binomial distribution in B. is shown for three different values of p. From Moss and Moczydlowski (1995).

Although the fine points of the Katz theory are still under discussion, most workers agree that it forms an adequate basis for understanding synaptic transmission at neuromuscular junctions. We consider whether or not it can be extended to synapses within the central nervous system in the next section.

Anatomy of central synapses.

Endplates at the neuromuscular junction occur at the terminations of motoneuron axons upon muscle cells. By contrast, central synapses occur between two or more neurons in the central nervous system and can involve any parts of the interacting neurons (Fig. 6-6). Synapses between the axon of one neuron and the soma or dendrite of a second are the most common, but synapses can occur between a pair of axons (*axoaxonic synapses*), a pair of dendrites (*dendrodendritic synapses*) or, less frequently, between a pair of somata (*somasomatic synapses*). Relatively complex assemblages of synapses are often seen. In some instances, these involve reciprocal relationships so the two elements in the synapse are pre- and postsynaptic to each other. In other cases, three elements interact in a *triadic relationship*. In still other cases, many elements interact in a synaptic *nest* or *glomerulus*.

Synapses effected by the axon of one neuron on another typically involve an axonal arbor of the presynaptic neuron which is formed by the axon of the neuron branching several times (Fig. 6-10). Axonal arbors are relatively thin and unmyelinated. They can form one or more synaptic boutons or a series of swellings, or *varicosities*, that occur sequentially, or

en passant, on the axon. In the latter case, one axon may make multiple synaptic contacts upon the postsynaptic neuron. These geometric complexities pose difficulties for the kind of analysis carried out for neuromuscular junctions. In the peripheral nervous system, the axon often makes one large synaptic terminal on a muscle cell. Activation of the motoneuron axon elicits a synaptic current at only one locus on the muscle fiber. The recording electrode can be placed adjacent to the presynaptic element to minimize electrotonic filtering of the EPP. By contrast, an axon in the central nervous system that forms *en passant* synapses along the dendrite of a postsynaptic neuron will elicit an asynchronous sequence of synaptic currents in the postsynaptic cell. The voltage transient recorded at the soma is a compound event generated by many independent PSCs

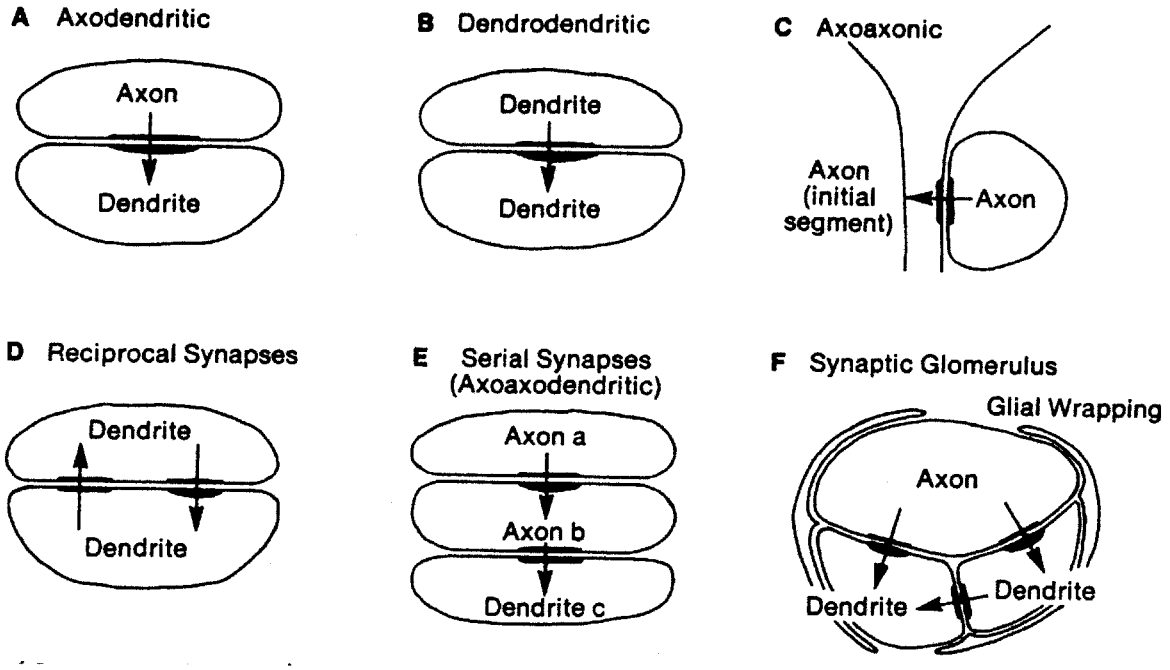

Figure 6-9. Synaptic arrangements. Six different sets of synaptic relationships are diagrammed. A through D involve synapses between two neurons. E and F involve more complex relationships between several neurons. From Shepherd (1979).

occurring over some time window, each of which has been subjected to a different amount of electrotonic filtering.

Presynaptic terminals vary significantly in shape and size between different axons and different species. Many terminals are small fusiform structures, measuring 1 μm or less along their long axes. Others are approximately spherical in shape and measure 2 or 3 μm in diameter. Extreme cases are large, bag shaped presynaptic terminals which measure 5 to 8 μm in diameter. Examples of these are the synapses made by mossy fibers on the proximal dendrites of CA3 pyramidal cells in the hippocampus or large terminals occuring in the granule cell layer of the cerebellum. In some cases, presynaptic elements are flattened along one side where they are apposed to a postsynaptic soma or dendrite. In other cases, they are invaginated by the heads of dendritic spines. In still others, they encase a postsynaptic element such as a soma. This occurs frequently in the auditory and electrosensory systems where a presynaptic element forms a so-called *calyceal ending* shaped like a vase or calyx.

The general features of the ultrastructure of central synapses (Fig. 6-11) resemble those of the neuromuscular junction. The presynaptic elements contain synaptic vesicles and structures that appear dark, or *electron dense*, in electron micrographs and are related to the mechanisms that mediate vesicle release. Each of the features varies between neurons in ways that appear related to the functional properties of the synapses. Vesicles vary in size and shape both within and between the presynaptic elements of synapses. Most contain two or more populations of vesicles.

One population is made up of vesicles that are clear, or *electron lucent*, in electron micrographs. These contain so-called classical neurotransmitters that evoke PSPs in the postsynaptic element with a relatively short latency.

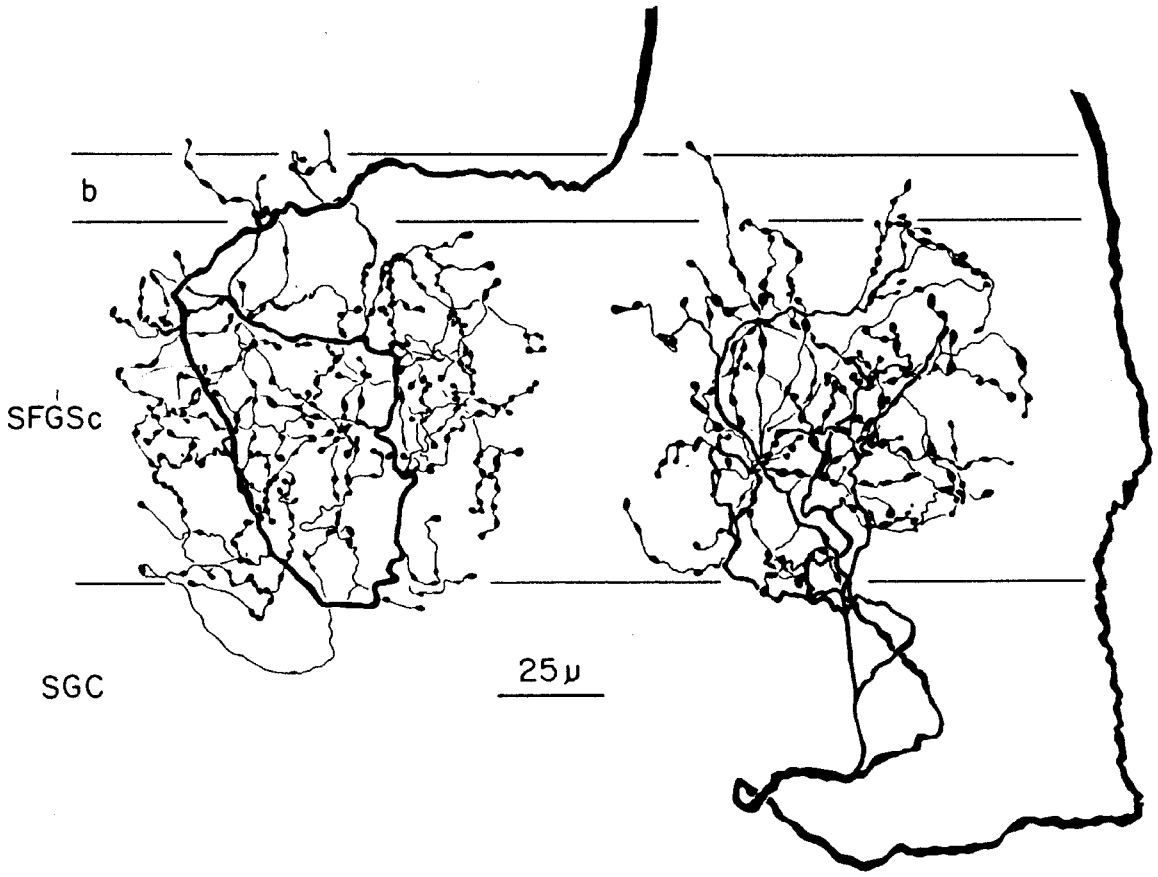

Figure 6-10. Axonal arbors. Two axons form terminal arbors in the superficial layers of the optic tectum of a snake. The axons were filled with HRP for visualization. Boundaries of layers are indicated to the left of the drawing. From Dacey and Ulinski (1986).

Classical neurotransmitters include both excitatory transmitters, such as acetylcholine and *glutamate,* and inhibitory transmitters, such as γ-aminobutryic acid (*GABA),* and *glycine*. Clear vesicles are uniformly round in cross section, but vary in size in material prepared for electron microscopy without fixation. The process of fixation alters vesicle morphology so

relatively small vesicles often become flattened. They appear as a mixture of round or ellipsoidal profiles in random thin sections and are described as *pleomorphic* or having many shapes. Large round vesicles in unfixed material retain their shape throughout the fixation process. The reasons for the different reactions of small clear and large clear vesicles to fixation are not fully understood, but there is a strong correlation (which is also not understood) between vesicle morphology, and the neurotransmitter contained in the vesicle. Neurotransmitters that have an excitatory effect at the postsynaptic membrane tend to occur in large clear vesicles while neurotransmitters with inhibitory effects tend to occur in clear pleomorphic vesicles. Although the resulting correlation between structure and function should be taken cautiously because the underlying causality remains unknown, vesicle morphology is often used to infer whether synapses visualized in electron micrographs are excitatory or inhibitory. Synapses formed from presynaptic elements with large clear vesicles are hypothesized to be excitatory and those with clear pleomorphic vesicles are hypothesized to be inhibitory. In addition to a population of clear vesicles, most presynaptic elements contain one or more populations of vesicles with larger diameters that contain *dense cores*. These vesicles contain peptides that serve as neurotransmitters or, in some cases, *neuromodulators* that modify the response of the postsynaptic element to the classical transmitter. The dense core is formed from the biochemically stabilized neuromodulator.

Central synapses do not show the bar-shaped active zones present in motoneuron terminals. There is, instead, a gridwork of presynaptic proteinaceous material along the presynaptic membrane. The gridwork is

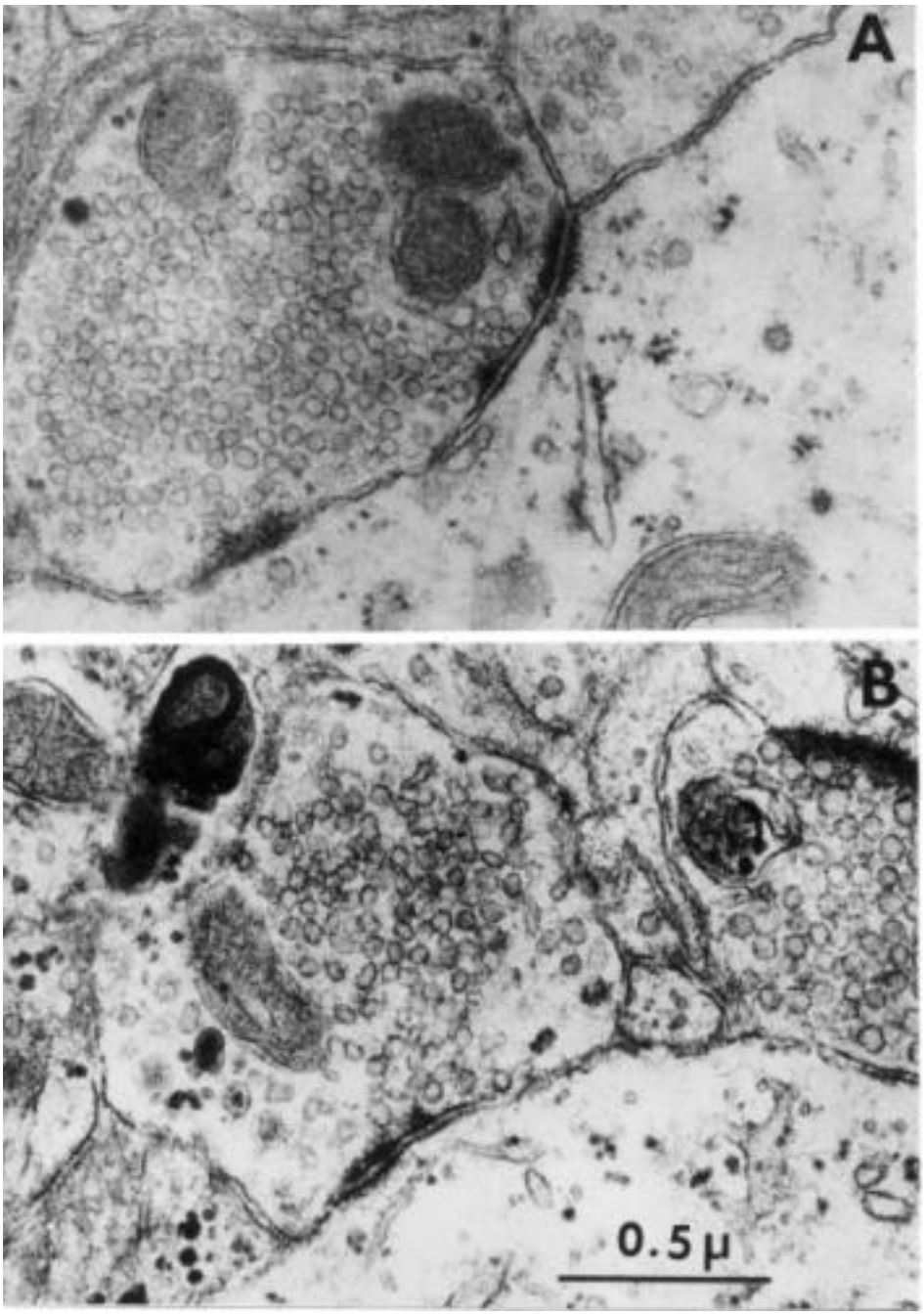

Figure 6-11. Ultrastructure of a central synapse. A. Electron micrograph of an asymmetric synapse. The presynaptic element contains round clear vesicles and a few dense cored vesicles. The active zones have well developed synaptic densities. B. Electron micrograph of a symmetric synapse. Clear synaptic vesicles are pleomorphic, with some showing definite flattening. The active zone has relatively little dense material.

composed of short bars arranged into triangles and individual vesicles nestle into the spaces formed by the bars. Other synapses, such as some formed between neurons in the retina, have vertically oriented slabs of presynaptic proteins. These resemble ribbons when cut in cross section and synapsesformed from elements that contain them are called *ribbon synapses*. The ribbons also serve to control vesicle release, but the vesicles aggregate along either face of the ribbon.

The synaptic cleft at the neuromuscular junction is relatively wide and contains a distinct basal lamina composed of proteins that bind acetylcholinesterase. The cleft at central synapses is generally narrower and contains less intracleft material. Central synapses can be placed into two groups based on the widths of their synaptic clefts (Fig. 6-12). Some have relatively narrow clefts, about 1,300 nM wide, while others have wider clefts, about 1,600 nM wide. These variations are related and some general patterns emerge when the morphology of many synapses are surveyed. The patterns were recognized shortly after the ultrastructure of synapses was visualized with the electron microscope. One common terminology is to recognize *asymmetric* and *symmetric synapses*. Asymmetric synapses have a postsynaptic density that is markedly thicker than is the presynaptic density. They have a relatively wide synaptic cleft and typically have clear, round vesicles in the presynaptic terminal. Assuming that clear, round vesicles are associated with an excitatory effect at the postsynaptic element, asymmetric synapses would generate EPSPs. Symmetric synapses have postsynaptic densities that are approximately the same thickness as the presynaptic density. They have a narrower cleft and clear, pleomorphic vesicles. They would generate IPSPs.

Central synapses are more difficult to study than are neuromuscular junctions, and the technical difficulties associated with recording from central neurons made it difficult to investigate the validity of the Katz

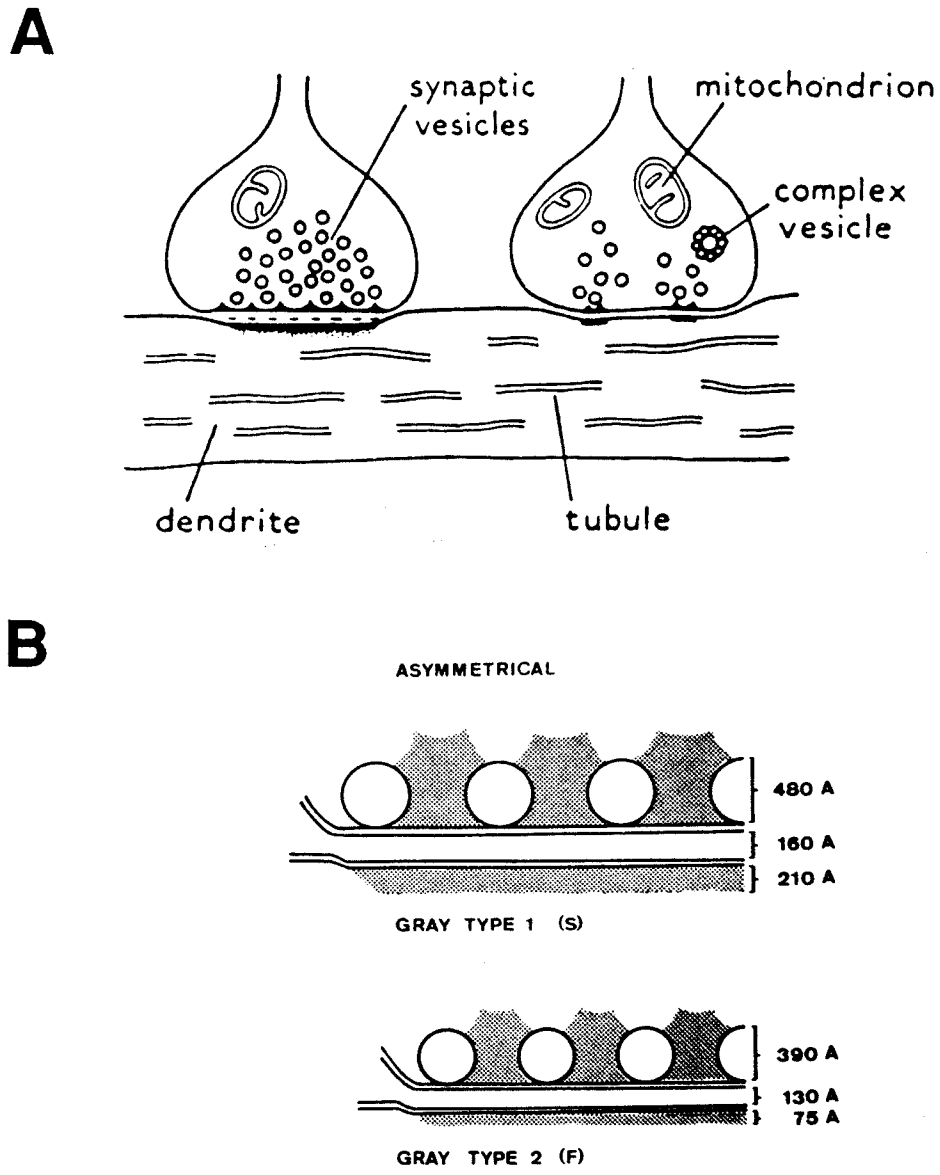

Figure 6-12. Symmetric and asymmetric synapses. From Akert et al. (1972). A. Diagram of an asymmetric (left) and a symmetric (right) synapse between axon terminals and a dendritic shaft. Compare these to the electron micrographs in Figure 3-22. B. Details of the active zones in asymmetric and symmetric synapse.

theory until relatively recently. Progress has depended upon the development of new technical approaches (Korn and Faber, 1991; Stevens, 1993).

Studying PSPs and PSCs in central synapses

Deconvolution methods. One difficulty that plagued early attempts to characterize central synapses is that PSPs recorded at central synapses were often not much larger than the noise present in the recording system because the first generation of intracellular recording electrodes had low resistances and low signal-to-noise ratios. It was not too difficult to recognize and measure large synaptic potentials, presumably resulting from the release of many vesicles. However, miniature events that could be associated with spontaneous release of single vesicles were ususally embeded in background noise. One approach to this difficulty is to carry out a *deconvolution analysis* based on some of the same conceptual approaches we talked about above in the context of predicting the effects of electrotonic filtering (Fig. 6-13). In that case, we thought of the neuron as a filter and viewed the synaptic current as filtered by the cell membrane. The impulse response function for the neuron was convolved with the input current to predict the shape of the filtered PSP. In this case, we consider the noise inherent in the recording apparatus as a filter and view PSPs as filtered through the noise. The waveform recorded by the electrode is obtained by convolving the untainted synaptic potential with a function that describes the noise. We can obtain a description of the noise by simply recording from the neuron in the absence of synaptic activity. One common form of noise is *Gaussian noise*. That is, a sequence of membrane

fluctuations with an amplitude distribution adequately described by a Gaussian distribution function. The knowns in this case are the noise function and the shape of the recorded waveform. What we want to find is the shape of the underlying PSP. Mathematically, we do the opposite of evaluating the convolution integral, a process known as *deconvolution*.

Another application of deconvolution techniques is to reconstruct the amplitude histograms of PSPs (Fig. 6-14) recorded in a noisy record (Redman, 1990). The methods used for this process can be technically elaborate, but we can consider a simple case to see how the process works. The case involves Gaussian noise specified by the mean amplitude and standard deviation of a section of the recording that appears to be free of synaptic activity (Fig. 6-15). So, we have a noise function, $N(v)$, that is given by

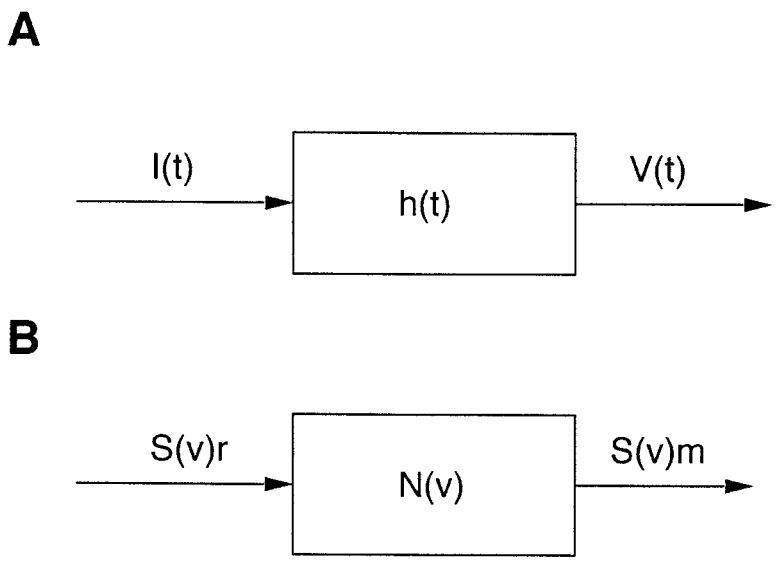

Figure 6-13. Convolution versus deconvolution. The essential features of convolution and deconvolution are compared. In convolution, an input function is convolved with a second function to obtain the output function. In deconvolution, the input function is estimated from the output function and a description of the system.

(6-26) $$N(v) = \frac{1}{\sigma\sqrt{2\pi}} Exp\left[-\frac{(v-\mu)^2}{2\sigma^2}\right]$$

where v is the membrane potential. An important point is that deconvolution analysis requires some assumption about the distribution of PSP amplitudes uncontaminated by noise. Let's assume that PSP amplitudes are quantized and occur as a series of discrete lines in an amplitude histogram. This situation can be represented mathematically as a sum of Dirac delta functions:

(6-27) $$S_r(v) = \sum_{i=1}^{n} \delta(v_i)$$

where $S_r(v)$ is the probability density function of the real amplitudes of the PSPs. With a knowledge of the form of the noise distribution and an assumption about the amplitude histogram, we predict the distribution of measured PSP amplitudes, $S_m(v)$, by convolving the uncontaminated distribution with the noise distribution

(6-28) $$S_m(v) = \int_0^x N(u)S(v-u)du \quad .$$

The integral is easy to evaluate because of a special property of the delta function

(6-29) $$\int_{-\infty}^{+\infty} y(x)\delta(x_i)dx = y(x_i) \quad .$$

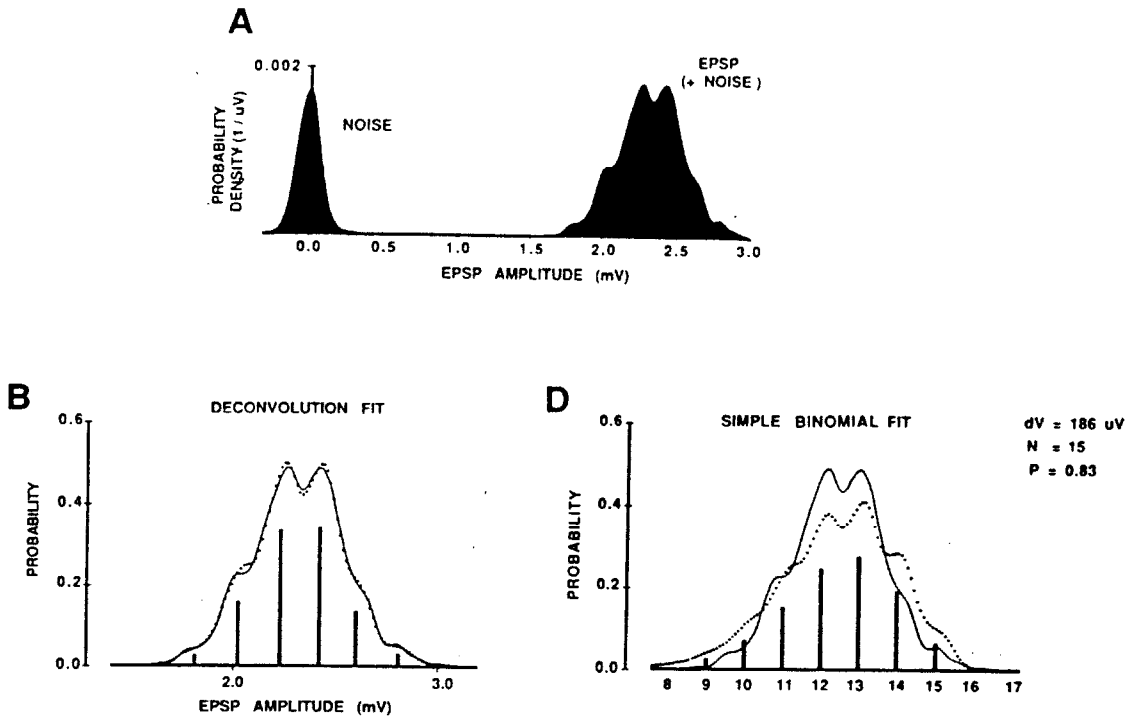

Figure 6-14. Deconvolution analysis of amplitude histograms. A. Histograms of the amplitude of membrane noise and of EPSPs contaminated by noise are used for a deconvolution analys. B. Assumming that the underlying probability density function is binomial, the deconvolution fits the EPSP amplitude histogram with a sum of six Gaussian functions. C. The result in B can be compared to the fit obtained using a simple binomial function and no effort to remove noise from the histogram of EPSP amplitudes. From Walmsley et al. (1985).

where $y(x)$ is a function of $x_i$and x_i is a specific value of x. Evaluation of the convolution integral leads to the prediction that the histogram of measured amplitudes is a sum of Gaussian functions.

(6-30) $$S_m(v) = \sum_{i=1}^{n} \frac{1}{\sigma\sqrt{2\pi}} Exp\left[-\frac{(v-\mu_i)^2}{2\sigma^2}\right] .$$

There are standard methods in the statistics literature for fitting sums of Gaussian functions to data sets, so we can estimate the parameters of the distributions by collecting a suitably large sample of the membrane potential

during synaptic activity, measuring the amplitudes of the events in the record and fitting Gaussian functions to the data set. The parameters, μ_i, specificy the amplitudes of the peaks in the histogram of uncontaminated PSP amplitudes. Deconvolution analysis is not limited by this particular assumption about the shape of the uncontaminated amplitude distribution and the review by Redman (1990) should be consulted for references on how to proceed with deconvolution analysis for more complex distributions.

This approach was used by Jack et al. (1981) to study the waveforms of PSPs elicited in motoneurons by the synapses of Ia afferents (Fig. 6-15). They recorded samples of EPSPs evoked by electrical activation of Ia afferents in cat spinal motoneurons and then filled both the motoneuron and the afferent with HRP. They were then able to determine the number of synaptic contacts made by the afferent upon the motoneuron by looking for points of close apposition between the afferent and motoneuron. In one case, the afferent made four synaptic contacts upon two dendrites. Analysis of the EPSPs showed that the amplitudes of the EPSPs fluctuated between large and small amplitude EPSPs, which presumably resulted from random activation of one or the other collaterals of the afferent. They obtained a sample of the baseline noise from the recordings and fit the resulting distribution with a Gaussian noise function. Using the assumption that the underlying real distribution of EPSP amplitudes was two delta functions, they were able to fit the histogram of noisy EPSP records with a sum of two Gaussian functions. The review by Redman (1990) provides further examples of this approach, but it should be noted that analysis of PSP data sets from central synapses often require a *two-step deconvolution process* in which individual PSPs are identified by a deconvolution that

removes the noise from the trace in the first step. The ensemble of PSPs are then fit to an amplitude histogram by a deconvolution analysis using one or more model distribution functions in the second step.

Application of the Katz theory to central synapses

The Katz theory predicts that amplitude histograms of PSPs should have distinct peaks resulting from the release of one or more quanta of transmitter. Each quantum is produced by the transmitter packaged in one vesicle. There is some variance in amplitude around each of these peaks due to inevitable variations in the number of molecules packaged in the vesicle. The mean amplitudes of the larger peaks should be integral multiples of the amplitude of the smallest peak, which results from release of single vesicles. For the neuromuscular junction, the smallest PSPs could be recorded in the presence of zero calcium and were attributed to spontaneous release of vesicles.

We also learned in the preceding section that attempts were made to overcome the signal/noise problems associated with early intracellular recording methods using deconvolution methods. The quality of intracellular electrodes gradually improved and the advent of high resistance patch-clamp electrodes made it possible to detect even small amplitude PSPs. Some work has been done *in vivo* in intact nervous systems, but most studies of central transmission are now done with patch clamp methods and *in vitro* slices. The paradigm is typically to evoke PSPs by electrical stimulation of afferent fibers and then repeat the study with tetrodotoxin (TTX) added to the bath in the recording chamber. TTX is a poison derived from puffer fish

that blocks sodium channels in the afferent fibers, and consequently prevents the generation of action potentials. Any PSPs that survive bath application of TTX can, thus, be attributed to spontaneous vesicle release. As predicted, bath application of TTX usually reduces the amplitudes of PSPs recorded from central neurons.

The first attempts to evaluate the Katz hypothesis for central neurons were carried out by Motoy Kuno at Duke University (Kuno, 1964, 1971). He used an *in vivo* cat preparation and stimulated Ia afferents in the spinal nerves. He could characterize the Ia afferents by their responses to stretching the leg muscles and recording intracellularly from both spinal motoneurons and neurons in a spinal cord structure called the *nucleus dorsalis* or *Clarke's column*. Neurons in the nucleus dorsalis receive monosynaptic inputs from branches of the Ia afferents. Their efferent axons course up the spinal cord to the brain and synapse in the cerebellum forming the *dorsal spinocerebellar tract*. Comparison of EPSPs in motoneurons and neurons in nucleus dorsalis is interesting because individual Ia axons have branches that synapse on either motoneurons or neurons in nucleus dorsalis. However, the terminals formed by the two branches are not the same. Those synapsing on neurons in nucleus dorsalis are larger than those synapsing on motoneurons. Amplitude histograms constructed for EPSPs recorded from the two groups of neurons varied in amplitude from 0.1 to 0.9 mV and showed some tendency to contain peaks (Fig. 6-16). These peaks could not be adequately fit by a Poisson distribution, and so differ from the distributions found by del Castillo and Katz for the neuromuscular junction. However, these workers were limiting vesicle release by working in a low calcium bath in a way that is not possible in an

intact nervous system. It was, then, not surprising that the amplitude histograms obtained in cats could be fit with binomial distributions. This implies that the probability of release at the central synapses was higher than in the neuromuscular junction. Kuno also found that the mean quantal content was much smaller than at the neuromuscular junction. This also was not surprising because electron microscopic studies of Ia afferents show they have many fewer vesicles than do neuromuscular junctions. Ia terminals on nucleus dorsalis neurons are larger and have more vesicles than do those on motoneurons and the mean quantal content for PSPs recorded in nucleus dorsalis neurons was higher than for PSPs recorded in motoneurons. This early study suppported the Katz theory with the understandable modifications that the probability of release was higher in the intact animal than at the neuromuscular junction and the mean quantal content was smaller in smaller terminals. However, most workers recognized the technical difficulties involved in collecting and analysing the data and reserved judgement about the success of the theory.

Kuno's work on Ia synapses upon motoneurons and DSCT neurons was redone as deconvolution methods were introduced (Jack et al., 1981; Redman and Walmsley, 1983; Walmsley et al. 1985, 1988). An additional advance, discussed above, was that it became possible to visualize both the presynaptic Ia afferent and the postsynaptic neuron by recording from both elements and filling them with HRP. This allowed knowledge of the number of synaptic contacts effected by the afferent and their position on the neuron relative to the soma. Discrete, quantal-like peaks were usually not obvious in the histograms of EPSP amplitiude. However, deconvolution procedures were then used to construct histograms of the peak voltages of

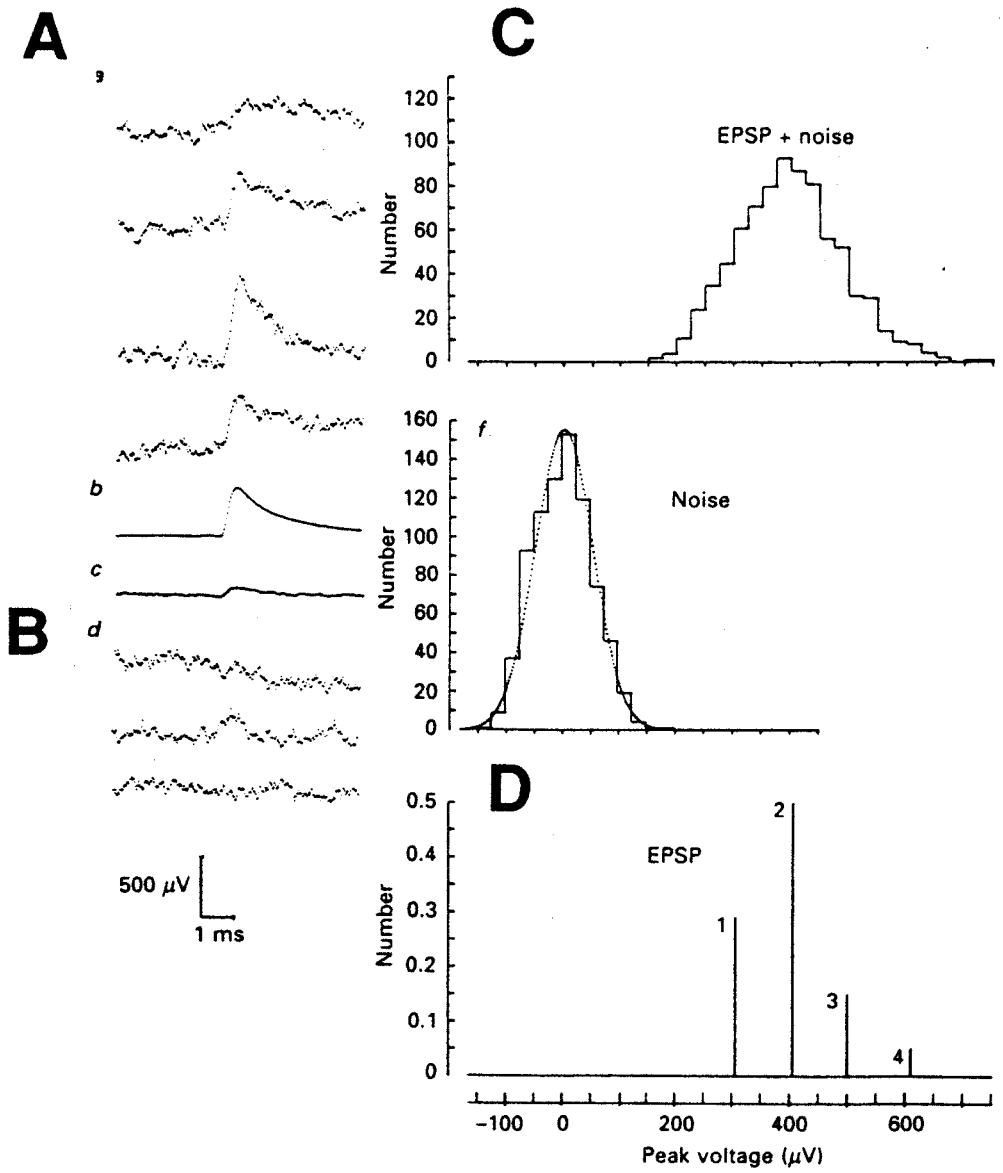

Figure 6-15. Deconvolution anlysis of EPSPs from cat spinal motoneurons. A. Examples of EPSPs. B. Examples of segments of recordings in which no EPSPs are evident, to provide a noise sample. C. Amplitude histogram of EPSPs with noise (upper histogram) and noise (lower histogram). D. Amplitude histogram resulting from the deconvolution analysis. From Jack et al. (1981).

EPSPs evoked by activation of the Ia afferents. The results tended to show a sequence of discrete amplitudes. The observed histograms could be

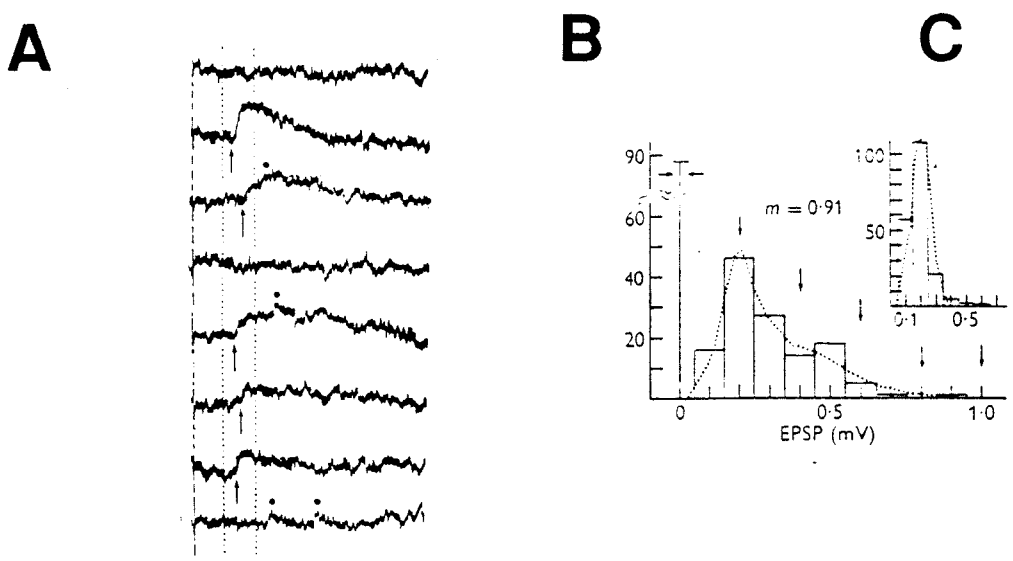

Figure 6-16. Amplitude histograms for EPSPs in motoneurons. A. Sample of EPSPs evoked in cat spinal motoneurons by activation of Ia afferents. B. Histogram of amplitudes of evoked EPSPs and best-fit binomial distribution. C. Histogram of spontaneous EPSPs and best-fit Gaussian function. From Kuno (1964).

interpreted as a sum of Gaussian distributions with means equal to these peaks. A second finding was that the probabilities associated with the peaks in the reconstructed histogram could usually not be described by simple binomial or Poisson distributions. Rather, the probabilities associated with each discrete amplitude were best described by a *compound binomial distribution*. This implies that different probabilities of release are associated with different release sites, and raises the possibility that a quantal EPSP is generated when transmitter is released by an individual synaptic bouton. The probability of release can be $p = 1$ at some boutons and $p < 1$ at others. In some instances, $p = 0$.

In the Katz theory, n in the binomial equation was interpreted to be the number of *vesicles* in one terminal that are available for release. A tacit

assumption in this analysis was that each bouton on the Ia terminal had a single release site. However, the suggestion stemming from the work on motoneurons and DSCT neurons was that n was equal to the number of *boutons* activated by the Ia afferent.

This line of thought was developed and modified to include the possibility that a bouton can have more than one release site by Henri Korn, Donald Faber and colleagues in their work on Mauthner neurons in goldfish (1991). *Mauthner neurons* are a relatively rare example of identified neurons in vertebrates (Fig. 6-17). They are found in the hind brain of all aquatic vertebrates and are involved in generating rapid escape movements in response to unexpected events in the water. Each goldfish has a pair of Mauthner neurons, one on each side of its rostral hindbrain. Each neuron in the pair has a large soma and large lateral and medial dendrites. The cell receives a remarkable variety of chemical and electrical synapses which have been carefully characterized by both anatomical and physiological methods (Faber and Korn, 1978). Many of the afferents are large enough to easily impale with microelectrodes, so Faber and Korn were able to stimulate and fill individual afferents while recording from a Mauthner cell. Results obtained by stimulating saccular afferents originating in the inner ear and an inhibitory interneuron were comparable. Amplitude histograms of the evoked EPSPs and IPSPs sometimes (but not always) showed discrete peaks (Fig. 6-18). Histograms reconstructed using a two-step deconvolution technique could be described by a compound binomial distribution. The binomial n values obtained from fits for individual Mauthner cells could then be compared to the number of presynaptic boutons formed by the afferent on that particular neuron. The numbers of active zones in each bouton were

also determined by carrying out serial reconstructions of the individual boutons after the recording session was completed. The analysis showed a strong correlation between the value of binomial n and the number of active zones. Some cells had n values larger than the number of boutons, but many had n values equal to the number of boutons. Some boutons had more than one active zone, but many had a single active zone. The original idea that n is the number of available vesicles in a single bouton was replaced with the idea that n is the number of active zones present in the several boutons present on an afferent terminal. Each active zone releases vesicles with a probability, p, which varies from bouton to bouton. This idea is called the *single vesicle hypothesis* (Fig. 6-20). It implies that the active zone somehow regulates vesicle release so that an individual active zone can release one, and only one, vesicle when it is activated. The single vesicle hypothesis has not been confirmed for all synapses, so it remains controversial.

The Ia afferent and Mauthner cell systems provide the technical advantage of allowing direct comparisons between PSP amplitude histograms for an individual neuron and the number and morphology of boutons contacting that same cell. It is difficult to establish the same kinds of structure-function relationships for most central neurons, and attempts to understand the amplitude histograms of PSPs or PSCs in, for example, mammalian cortical preparations tend to produce equivocal or controversial results. The best quality data are collected using contemporary patch-clamp

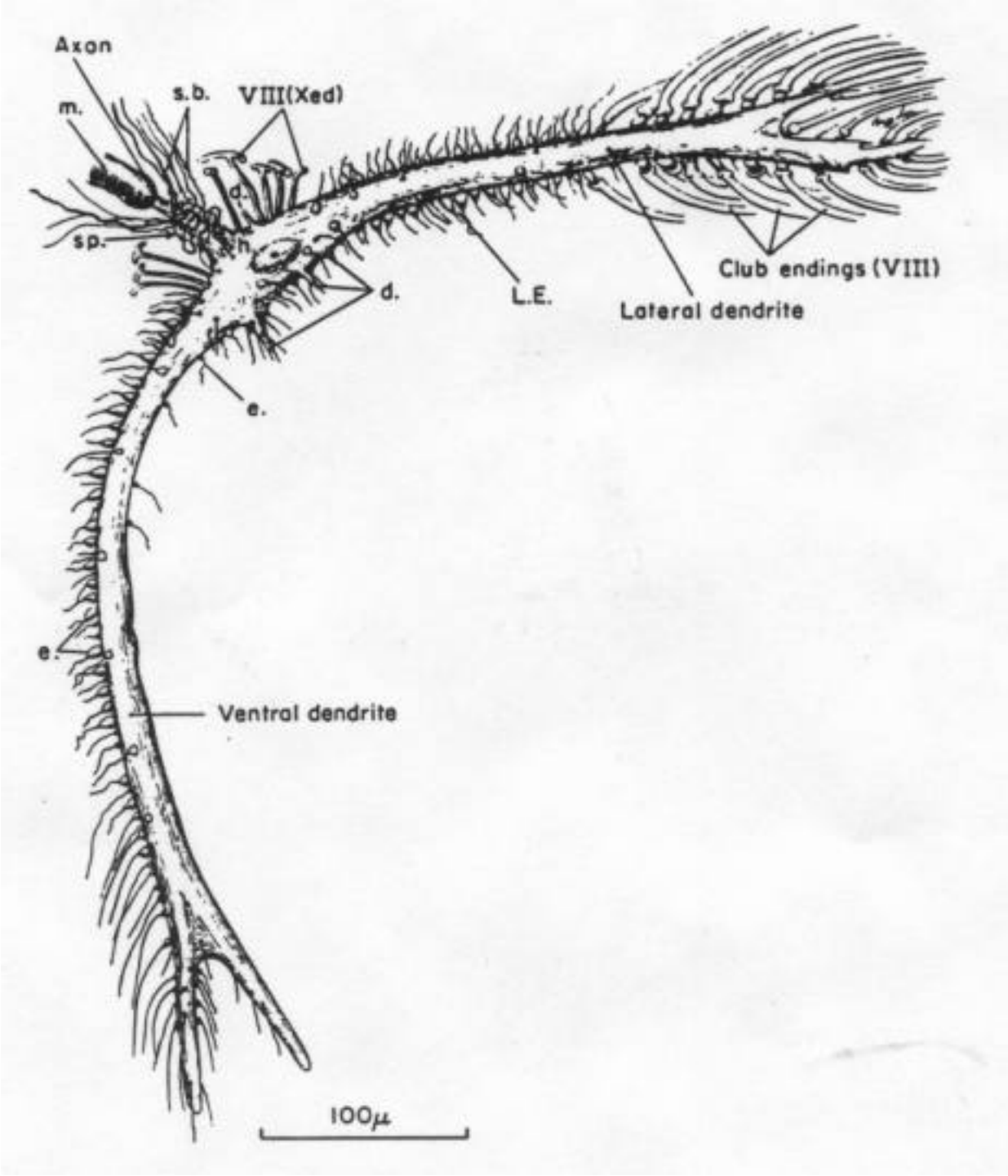

Figure 6-17. Mauthner neuron. A Mauthner neuron from the hindbrain of a goldfish. From Bodian (1952).

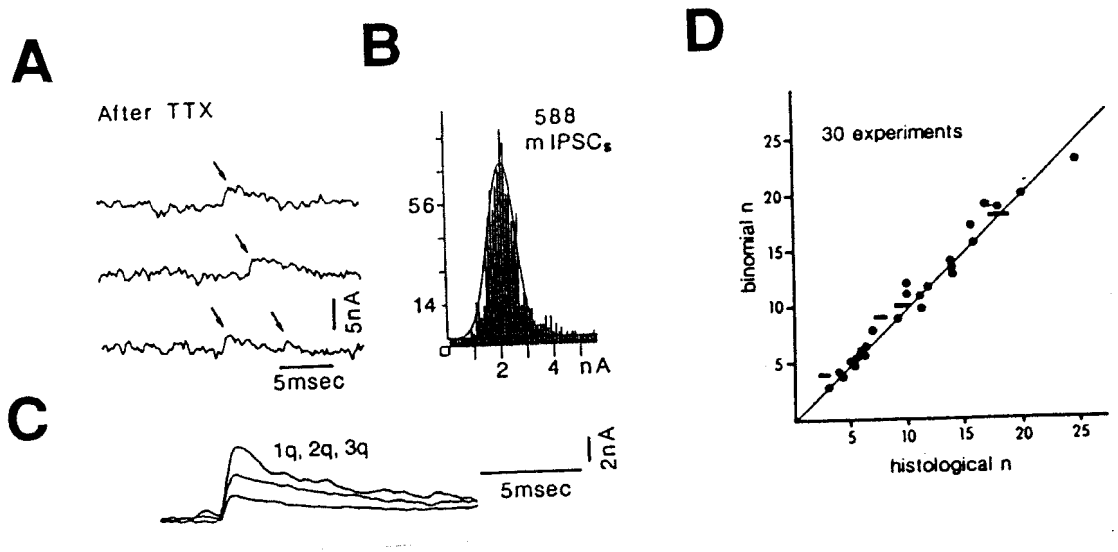

Figure 6-18. IPSPs in Mauthner neurons. A. Sample of IPSCs recorded from goldfish Mauthner neurons in tetrodotoxin to block action potential-dependent release of neurotransmitter. B. Histogram of spontaneous IPSCs and best fit-Gaussian function. C. Examples of IPSCs produced by 1, 2 and 3 quanta of transmitter. D. Relation between the n value obtained from the best-fit binomial distribution and the number of active zones counted in histological sections. From Korn and Faber (1991).

methods and slice preparations. Results have been variable with some authors reporting the presence of quantal peaks in amplitude histograms and others being unable to find discrete peaks. Jonas et al. (1993) demonstrated quantal peaks in amplitude histograms of IPSCs recorded in failure to find clear quantal peaks is the study of Ulrich and Lüscher (1991) who recorded from spinal motoneurons in rat slices. Distinct quantal peaks were not clear in their histograms, but they attempted to correct for the spatial distribution of individual synapses over the surface of the neuron. Synapses located at greater distances from the somatic recording site would be expected to generate smaller amplitude PSCs and PSPs due to temporal dispersion of charge and electrotonic filtering. Differences in electrotonic distance from the soma would, thus, tend to obscure quantal peaks if they were present in the soma. Ulrich and Lüscher used shape

parameter plots of the kind discussed in Chapter 5 to correct for amplitude reduction in electrotonically remote synapses. Amplitude histograms using PSP amplitudes corrected for electrotonic distance showed discrete quantal peaks, and the authors concluded that synapses show quantal transmission even in the absence of quantal peaks in histograms of evoked events.

An interesting preparation that avoids the difficulties arising from the spatial distribution of synapses on geometrically elaborate central neurons is the synapse between an auditory fiber and neurons in the *anteroventral cochlear nucleus* (AVCN) of mammals. This nucleus is part of a complex of nuclei which are the first central station in the ascending auditory pathways. Axons in the auditory nerve carry information from the inner ear into the brain and synapse in the AVCN. Neurons in AVCN have large, spherical somata and reduced dendritic trees. Auditory nerve synapses form remarkably large presynaptic boutons that virtually encapsulate the spherical cells. These endings were described at the light microscopic level by Held and are referred to as *endbulbs of Held*. Electron microscopy shows they have many release sites, suggesting they are "high p synapses" with large release probabilities. They are excitatory synapses that use the excitatory amino acid, glutamate, as a neurotransmitter. Isaacson and Walmsley (1995) examined the release process at this synapse using a slice preparation of rat AVCN. They constructed amplitude histograms of both spontaneous EPSCs and EPSCs evoked by electrical stimulation of the auditory nerve (Fig. 6-21). The histograms did not show signs of quantal peaks. However, they were able to duplicate the paradigm introduced by del Castillo and Katz for the neuromuscular junction and record events under low probability of release conditions. The synapse had Poisson statistics under

these conditions. Evoked EPSCs had longer time courses than did spontaneous events and the time course of evoked events could be reproduced by convolving the time course of a unitary event with the probability of release function. They suggest that the release process is asynchronous for evoked EPSCs, which tends to obscure quantal peaks in the histogram of evoked events.

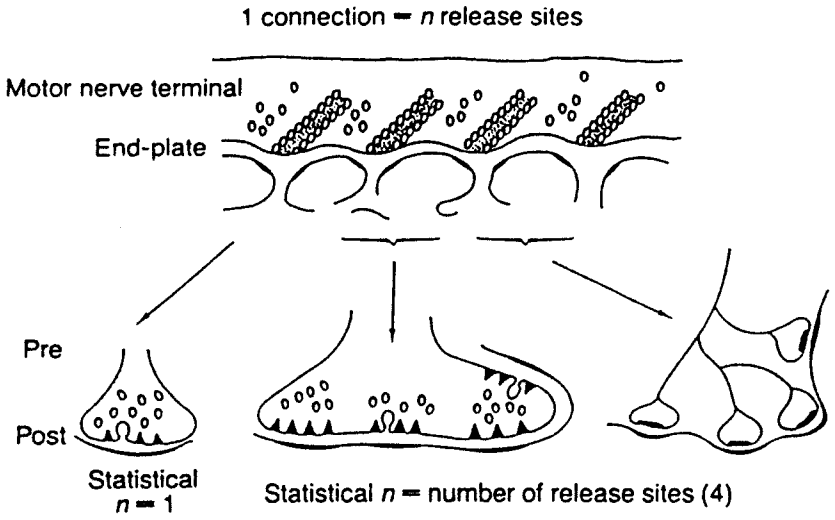

Figure 6-19. Single vesicle hypothesis. Comparison of the original formulation of the quantal hypothesis for a neuromuscular junction (top) and the single vesicle hypothesis for central synapses (bottom). At the neuromuscular junction, each action has multiple release sites. In central synapses, a given axon may have a single bouton with one release site or several release sites, or an axon may branch and give rise to several boutons, each of which has one release site. Each release site releases a single vesicle, so the number of release sites determines the maximum number of quanta that can be released by the axon. From Korn and Faber (1991).

The details of transmission at central synapses are not yet clear, but it appears that the general tenets of the Katz theory can be extended from the neuromuscular junction to central synapses. Quantal peaks are often difficult to demonstrate in central synapses, but this is probably a

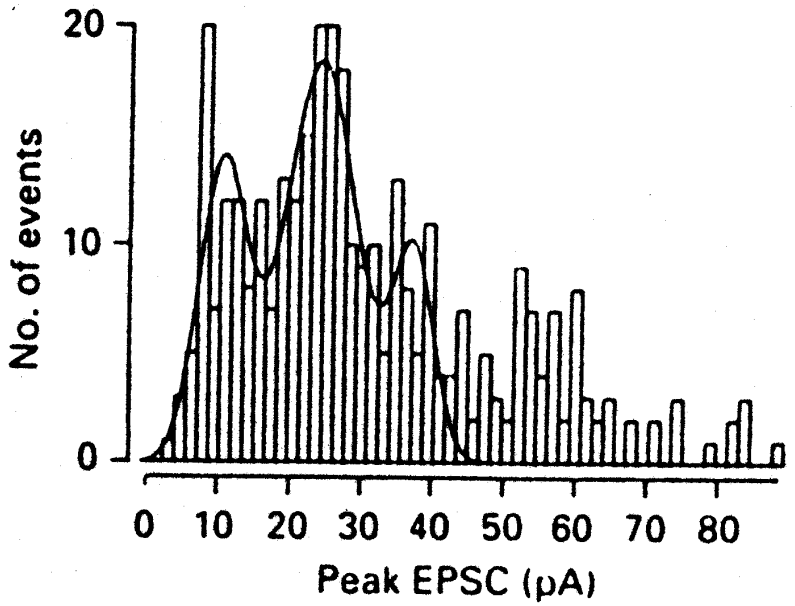

Figure 6-20. Amplitude histogram of EPSCs in hippocampal neurons An amplitude histogram of EPSCs from rat hippocampal neurons fit to a sum of three Gaussian functions. The histogram provides evidence for quantal peaks in central neurons. From Jonas et al. (1993).

reflection of sources of variability that were excluded from the original experiments at the neuromuscular junction by careful experimental design.

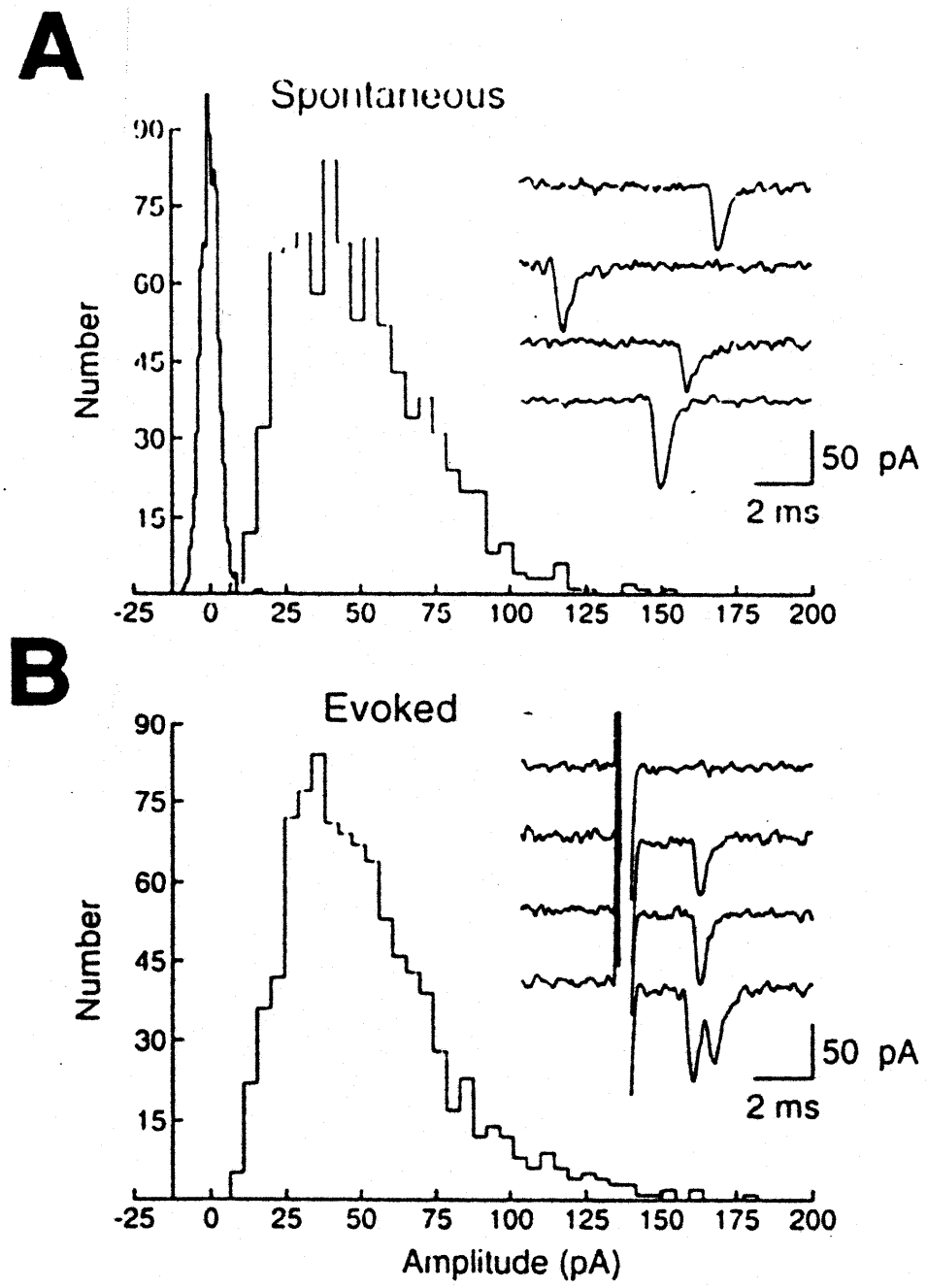

Figure 6-21. EPSCs in the anterior ventral cochlear nucleus. A. Amplitude histogram of spontaneous EPSCs recorded from neuron in the anterior ventral cochlear nucleus of rat brainstem. The narrow peak centered on 0 pA represents the noise level of the membrane. The larger histogram represents the amplitudes of spontaneously occuring EPSCs. Examples of individual EPSCs are shown in the inset. B. Amplitude histogram of EPSCs evoked by electrical activation of the auditory nerve. The inset shows examples of evoked responses. The dark vertical line that cuts across several traces is the stimulus artifact, that marks the onset of the stimulus. The histograms of neither the spontaneous nor the evoked responses show clear peaks attributable to quantal release. From Isaacson and Walmsley (1995).